

Detailed balance limit of silicon nanowire and nanohole array solar cells

Chenxi Lin* and Michelle L. Povinelli

Ming Hsieh Department of Electrical Engineering, University of Southern California,
3651 Watt Way, Los Angeles, CA, USA 90089-0106

[*chenxil@usc.edu](mailto:chenxil@usc.edu)

ABSTRACT

In this proceeding, we use optical modeling and detailed balance analysis to predict the limiting efficiency of nanostructured silicon solar cells based on vertically-aligned nanowire and nanohole arrays. We first use the scattering matrix method to study broadband optical absorption. By incorporating the calculated optical absorption into a detailed balance analysis, we obtain the limiting short circuit current, open circuit voltage, and power conversion efficiency of nanowire and nanohole solar cells. Results show that optimized nanowire and nanohole arrays of 2.33 microns in height have 83% and 97% higher power conversion efficiencies than a thin film with the same height, respectively. Furthermore, we find that the limiting power conversion efficiency is mainly determined by the short circuit current density, which is proportional to the broadband optical absorption.

Keywords: silicon nanowire array, silicon nanohole array, photonic crystal slab, absorption enhancement, light trapping, guided resonances, detailed balance limit, solar cells.

1. INTRODUCTION

Microstructured broadband absorbers hold great promise for cheaper, more efficient solar cells¹⁻¹⁶. Recent work has established that material microstructure can be tailored to achieve large absorption, even within a depth shorter than the optical absorption length. This approach, which we term *structural absorption engineering*, relies on carefully-designed microstructures to achieve efficient light trapping. Vertically-aligned silicon nanowire^{6, 17-25} and nanohole arrays²⁶⁻²⁹ provide model systems to study structural absorption enhancement. In our previous work²¹, we have shown theoretically that silicon nanowire array with optimized geometrical parameters have a higher broadband absorption than a thin film of the same height. This effect is due to a combination of anti-reflection and light trapping properties^{30, 31}, including the excitation of guided resonance modes. Similar conclusions have been found for silicon nanohole arrays²⁷. However, previous work calculated the *ultimate efficiency* of nanowire and nanohole structures, an upper bound on the efficiency that depends on optical absorption alone and does not consider the electrical properties of the cell. In this proceeding, we extend our previous work^{21, 28} to calculate a modified detailed balance limit on the efficiency of silicon nanowire and nanohole array solar cells.

The detailed balance limit of a solar cell³², also known as the “Shockley-Queisser limit”, is a fundamental physical limit on power conversion efficiency obtained by considering only intrinsic loss mechanisms. The original Shockley-Queisser analysis considered bulk solar cells. The short circuit current is proportional to the total number of photons above the band gap; it is assumed that all such photons are absorbed to generate electron-hole pairs. The value of reverse saturation current density is set by assuming that radiative recombination is the only recombination mechanism, and an ideal diode characteristic is used to describe the electrical properties of the solar cell.

Here we apply a modified detailed balance analysis to nanowire and nanohole geometries. As in Ref.33, we take into account the realistic optical absorption spectrum, rather than assuming perfect absorption above the band gap. In this way, we obtain a practical limiting efficiency for nanostructured thin film solar cells. We show that the detailed balance limit yields an efficiency for both optimized nanowire arrays and optimized nanohole arrays that is higher than a thin film with the same height. The optimal structural parameters for the arrays are similar to those obtained in our previous work^{21, 28}, which used optical modeling alone.

2. METHODS

Accurate optical modeling is used to determine an upper limit on solar cell efficiency, assuming perfect carrier collection and modeling the electrical properties of the cell as an ideal diode.

2.1 Optical modeling

Figure 1 shows vertically aligned silicon nanowire (a) and nanohole (b) arrays. Each array consists of a square lattice with lattice constant a . The diameter of the wire or hole is indicated by d . The filling ratio is defined as the fractional area occupied by Si in one unit cell, given by $(\pi d^2/4a^2)$ for nanowire arrays and $(1 - \pi d^2/4a^2)$ for nanohole arrays. We study an array thickness L of $2.33\mu\text{m}$, comparable to the thickness of silicon thin film solar cells³⁴. The thickness is shorter than the absorption length of crystalline silicon for wavelengths greater than $\sim 600\text{nm}$. The nanowire and nanohole structures are surrounded by air.

The structures are illuminated at normal incidence, as indicated by the red arrow. The electric field is polarized parallel to the direction between nearest-neighbor rods (or holes). The ASTM Air Mass 1.5 direct and circumsolar solar spectrum³⁵ is used to model the solar irradiance.

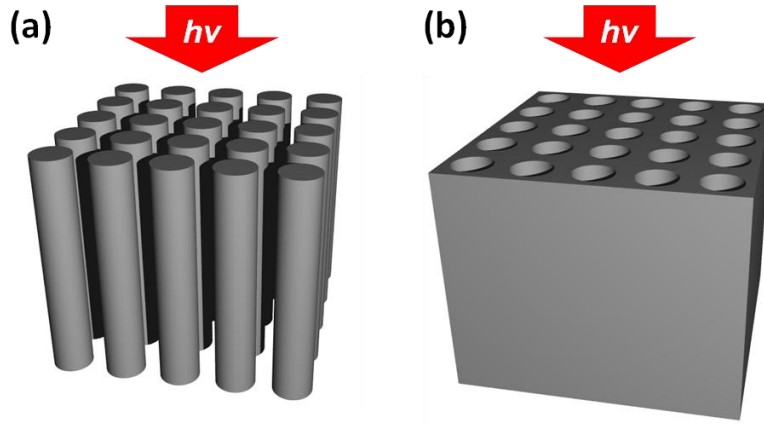


Figure 1 Square lattice nanowire (a) and nanohole (b) arrays.

We use a full-vectorial electromagnetic solver to calculate the wavelength-dependent absorptance, $A(\lambda)$, of the nanowire and nanohole structures. Simulations are performed using the ISU-TMM package³⁶, an implementation of the scattering matrix method³⁷. The refractive index and absorption coefficient of the silicon regions are set to the experimentally-determined, wavelength-dependent values for bulk silicon³⁸.

2.2 Modified detailed balance limit

The short circuit current can be related to the absorptance by

$$J_{sc} = \frac{e}{hc} \int_{310\text{nm}}^{\lambda_g} I(\lambda) A(\lambda) \lambda d\lambda \quad (1)$$

where $\lambda_g = 1127\text{nm}$ is the band gap of silicon, and the solar irradiance is negligible below 310nm . Eq. (1) assumes perfect carrier collection and so represents an upper bound on the short circuit current.

We use the J - V characteristic of an ideal diode to describe the electrical properties of the solar cell:

$$V(J) = \frac{k_B T}{q} \ln \left[\left(\frac{(J_{sc} - J) \times A_{illu}}{J_0 \times A_{junc}} \right) + 1 \right] = \frac{k_B T}{q} \ln \left[\left(\frac{J_{sc} - J}{J_0 \gamma} \right) + 1 \right], \quad \gamma = \frac{A_{junc}}{A_{illu}} \quad (2)$$

in which J is the current density of the solar cell, V is the voltage between the terminals of the cell, and J_0 is the reverse saturation current density. A_{illu} is the illumination area, and A_{junc} is the junction area. In planar thin films, γ equals unity. In nanostructured thin films, γ depends upon the specific junction geometry. Here we assume an *axial* p - n junction geometry, where the p and n regions are vertically stacked. Therefore, γ is equal to the filling ratio of the array.

We take the value of the reverse saturation current density to be [39]:

$$J_0 = \frac{2\pi q}{h^3 c^2} (n_T^2 + n_B^2) k_B T (2k_B^2 T^2 + 2k_B T E_g + E_g^2) \exp\left(-\frac{E_g}{k_B T}\right) \quad (3)$$

where n_T and n_B are the refractive indices of the superstrate and substrate of the solar cell, equal to 1 (air). For crystalline silicon with a band gap of 1.1eV at $T = 300\text{K}$, the value of J_0 is $5.4 \times 10^{-13} \text{ mA/cm}^2$.

By setting the total current $J = 0$, we obtain the open circuit voltage of the solar cell. Under the assumption that $J_{sc} \gg J_0$,

$$V_{oc} = V(J = 0) = \frac{k_B T}{q} \ln\left[\left(\frac{J_{sc}}{J_0 \gamma}\right) + 1\right] \approx \frac{k_B T}{q} \ln\left(\frac{J_{sc}}{J_0 \gamma}\right) = \frac{k_B T}{q} \ln\left(\frac{J_{sc}}{J_0}\right) - \frac{k_B T}{q} \ln \gamma \quad (4)$$

The power conversion efficiency is defined as

$$P.C.E = \frac{V_{mpp} J_{mpp}}{I_{in}} = \frac{V_{oc} J_{sc} FF}{I_{in}} \quad (5)$$

where V_{mpp} and J_{mpp} are the voltage and current density that maximize the power $J \times V(J)$, $FF \equiv V_{mpp} J_{mpp} / V_{oc} J_{sc}$ is the fill factor, and I_{in} is the incident solar power density. For the ASTM AM1.5 direct and circumsolar solar spectrum, I_{in} is about 900.14 W/m^2 .

For a given nanowire or nanohole structure, the power conversion efficiency can be determined numerically using Eq. 2 and the value of the short circuit current can be obtained from the optical simulation (Eq. 1).

3. RESULTS

Figure 2 shows calculation results for nanowire (a, c, e) and nanohole (b,d,f) arrays. We plot the short circuit current density, open circuit voltage, and power conversion efficiency for arrays with various structural parameters (lattice constant and filling ratio).

Figures 2 (a) and (b) show J_{sc} as a function of lattice constant and filling ratio for nanowire and nanohole arrays, respectively. In both cases, the maximum values of J_{sc} are obtained for lattice constants in the 600nm – 700nm range and moderate filling ratio (~ 0.5). The value of the short circuit current density is higher than that for a thin film with the same thickness. It is also higher than the value for a thin film with a single-layer Si_3N_4 AR coating.

Figures 2 (c) and (d) show V_{oc} as a function of lattice constant and filling ratio. V_{oc} increases with decreasing filling ratio for both nanowires and nanoholes. The variation in voltage is small ($<6\%$) over the range of parameters plotted. From Eq. (4), V_{oc} scales as $\ln(J_{sc}/\gamma)$, where γ is the filling ratio. J_{sc} depends on γ , as seen above in Figures 2(a) and (b). Thus, the value of the filling ratio that optimizes J_{sc} does not necessarily optimize V_{oc} . Inspection of Figures 2(a) and 2(c) reveals that this is the case only for nanowire arrays.

We found that the fill factor (Eq. 5) is approximately 86% over the range of lattice constants and filling ratios considered.

Figures 2 (e) and (f) show the power conversion efficiency. The optimal nanowire structure ($a=650\text{nm}$ and $d=520\text{nm}$) has an efficiency of 15.98%. The optimal nanohole array structure ($a=600\text{nm}$ and $d=480\text{nm}$) has an efficiency of 17.18%. These values are higher than for a silicon thin film with the same thickness (8.71%), and even for a thin film with an optimal single-layer Si_3N_4 AR coating (12.99%). The dependence of efficiency on lattice constant and filling ratio is very similar to the short circuit current (Figures 2(a) and (b)), which can be attributed to the much more significant variation in the short circuit current density than the open circuit voltage.

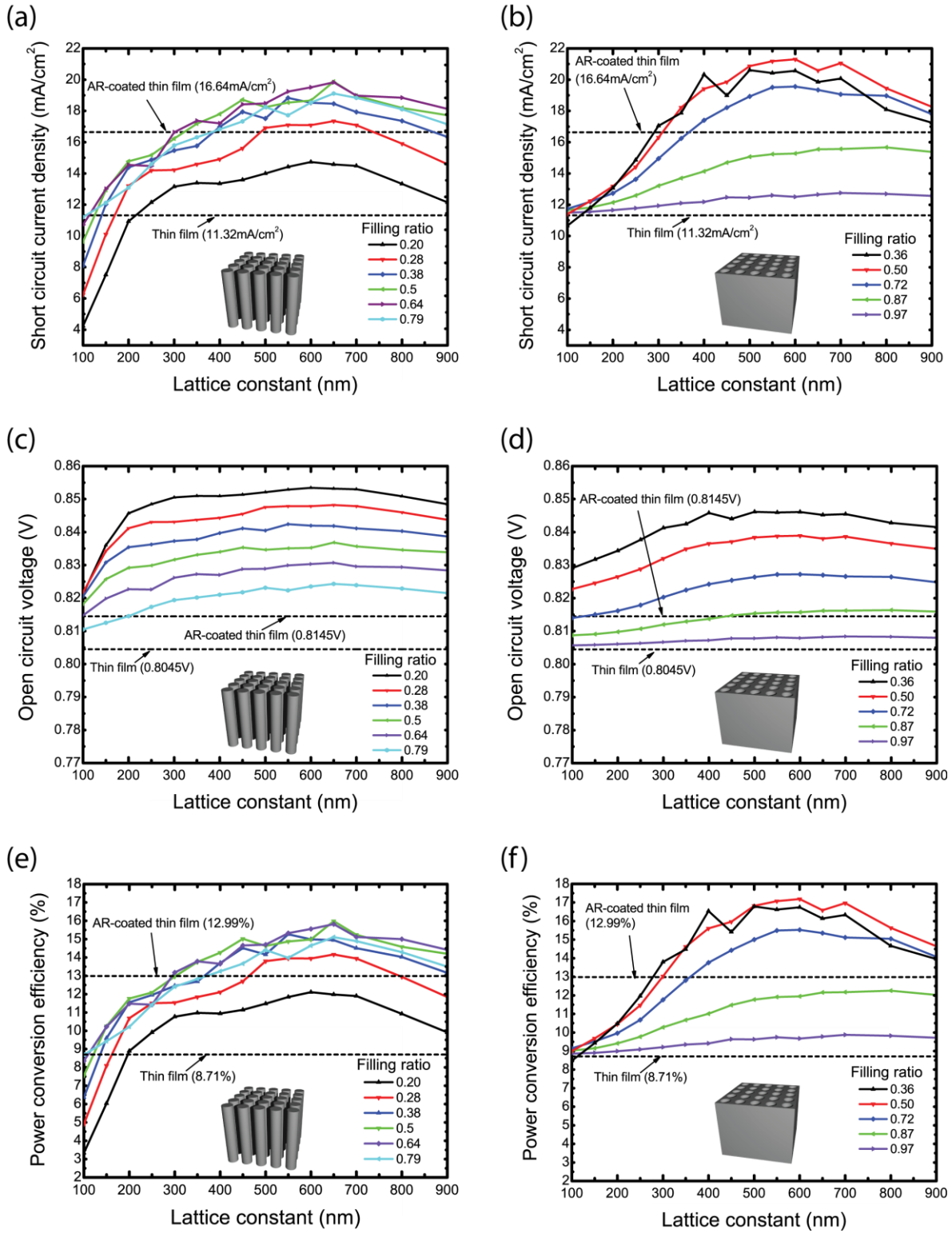


Figure 2 The dependence of solar cell characteristics on lattice constant and filling ratio for nanowire (a, c, e) and nanohole (b, d, f) arrays.

4. CONCLUSION AND DISCUSSION

To summarize, we have calculated an upper bound on the power conversion efficiency of silicon nanowire and nanohole solar cells. Our approach uses rigorous optical modeling in combination with a diode model of the current-voltage characteristics and assumes perfect carrier collection. The results show that both silicon nanowire and nanohole arrays with optimized structural parameters outperform an AR-coated thin film of the same thickness. Nanowire and nanohole arrays exhibit higher short circuit current, open circuit voltage, and power conversion efficiency. The dependence of the power conversion efficiency on the structural parameters of the arrays (filling ratio and lattice constant) largely follows that of the short circuit current, which is proportional to the broadband optical absorption.

We have assumed an axial p - n junction geometry in our analysis. Another possible geometry is the radial p - n junction³⁹. We have calculated the power conversion efficiency of radial junction geometries, and the values are generally lower. This is due to the increase in junction area, corresponding to $\gamma \gg 1$ in Eq. (4), which leads to a decrease in the open circuit voltage.

Further work may incorporate more detailed and realistic models of the electro-optical properties of the cell. Above, we have assumed a constant value of the reverse saturation current density, J_o (Eq. 3). Due to the possibility of emission enhancement in nanostructured films³³, J_o may vary with the filling ratio and lattice constant of nanowire or nanohole arrays. Moreover, we have assumed perfect carrier collection. It should be possible to place a stricter bound on power conversion efficiency using detailed device physics models^{29,40}.

ACKNOWLEDGEMENTS

The authors thank Ningfeng Huang for useful discussions. This work was funded by the Center for Energy Nanoscience, an Energy Frontiers Research Center funded by the U.S. Department of Energy Office of Science, Office of Basic Energy Sciences, under Award DE-SC0001013. Computing resources were provided by the USC Center for High Performance Computing and Communications.

REFERENCES

- [1] Lewis, N. S., "Toward Cost-Effective Solar Energy Use," *Science* 315(5813), 798-801 (2007).
- [2] Tsakalakos, L., "Nanostructures for photovoltaics," *Mat. Sci. Eng. R* 62(6), 175-189 (2008).
- [3] Sun, K., Kargar, A., Park, N., Madsen, K. N., Naughton, P. W., Bright, T., Jing, Y., and Wang, D., "Compound Semiconductor Nanowire Solar Cells," *IEEE J. Sel. Top. Quant.* 17(4), 1033-1049 (2011).
- [4] Zeng, L., Yi, Y., Hong, C., Liu, J., Feng, N., Duan, X., Kimerling, L. C., and Alamariu, B. A., "Efficiency enhancement in Si solar cells by textured photonic crystal back reflector," *Appl. Phys. Lett.* 89(11), 111111 (2006).
- [5] Bermel, P., Luo, C., Zeng, L., Kimerling, L. C., and Joannopoulos, J. D., "Improving thin-film crystalline silicon solar cell efficiencies with photonic crystals," *Opt. Express* 15(25), 16986-17000 (2007).
- [6] Hu, L., and Chen, G., "Analysis of optical absorption in silicon nanowire Arrays for photovoltaic applications," *Nano Lett.* 7(11), 3249-3252 (2007).
- [7] Zhou, D., and Biswas, R., "Photonic crystal enhanced light-trapping in thin film solar cells," *J. Appl. Phys.* 103(9), 093102 (2008).
- [8] Tumbleston, J. R., Ko, D.-H., Samulski, E. T., and Lopez, R., "Absorption and quasiguide mode analysis of organic solar cells with photonic crystal photoactive layers," *Opt. Express* 17(9), 7670-7681 (2009).
- [9] Li, J., Yu, H., Wong, S. M., Zhang, G., Sun, X., Lo, P. G.-Q., and Kwong, D.-L., "Si nanopillar array optimization on Si thin films for solar energy harvesting," *Appl. Phys. Lett.* 95(3), 033102 (2009).
- [10] Mallick, S. B., Agrawal, M., and Peumans, P., "Optimal light trapping in ultra-thin photonic crystal crystalline silicon solar cells," *Opt. Express* 18(6), 5691-5706 (2010).
- [11] Cao, L., Fan, P., Vasudev, A. P., White, J. S., Yu, Z., Cai, W., Schuller, J. A., Fan, S., and Brongersma, M. L., "Semiconductor Nanowire Optical Antenna Solar Absorbers," *Nano Lett.* 10(2), 439-445 (2010).
- [12] Yu, Z., Raman, A., and Fan, S., "Fundamental limit of light trapping in grating structures," *Opt. Express* 18(S3), A366-A380 (2010).
- [13] Peng, K. Q., Xu, Y., Wu, Y., Yan, Y. J., Lee, S. T., and Zhu, J., "Aligned single-crystalline Si nanowire arrays for photovoltaic applications," *Small* 1(11), 1062-1067 (2005).

- [14] Tsakalakos, L., Balch, J., Fronheiser, J., Shih, M. Y., LeBoeuf, S. F., Pietrzykowski, M., Codella, P. J., Korevaar, B. A., Sulima, O., Rand, J., Davuluru, A., and Rapol, U., "Strong broadband optical absorption in silicon nanowire films," *J. Nanophotonics* 1(1), 013552 (2007).
- [15] Muskens, O. L., Rivas, J. G., Algra, R. E., Bakkers, E., and Lagendijk, A., "Design of light scattering in nanowire materials for photovoltaic applications," *Nano Lett.* 8(9), 2638-2642 (2008).
- [16] Zhu, J., Yu, Z. F., Burkhard, G. F., Hsu, C. M., Connor, S. T., Xu, Y. Q., Wang, Q., McGehee, M., Fan, S. H., and Cui, Y., "Optical Absorption Enhancement in Amorphous Silicon Nanowire and Nanocone Arrays," *Nano Lett.* 9(1), 279-282 (2009).
- [17] Tsakalakos, L., Balch, J., Fronheiser, J., Korevaar, B. A., Sulima, O., and Rand, J., "Silicon nanowire solar cells," *Appl. Phys. Lett.* 91(23), 233117 (2007).
- [18] Stelzner, T., Pietsch, M., Andra, G., Falk, F., Ose, E., and Christiansen, S., "Silicon nanowire-based solar cells," *Nanotechnology* 19(29), 295203 (2008).
- [19] Garnett, E. C., and Yang, P. D., "Silicon nanowire radial p-n junction solar cells," *J. Am. Chem. Soc.* 130(29), 9224-9225 (2008).
- [20] Sivakov, V., G. Andrä, G., Gawlik, A., Berger, A., Plentz, J., Falk, F., and Christiansen, S. H., "Silicon Nanowire-Based Solar Cells on Glass: Synthesis, Optical Properties, and Cell Parameters," *Nano Lett.* 9(4), 1549-1554 (2009).
- [21] Lin, C., and Povinelli, M. L., "Optical absorption enhancement in silicon nanowire arrays with a large lattice constant for photovoltaic applications," *Opt. Express* 17(22), 19371-19381 (2009).
- [22] Li, J., Yu, H., Wong, S. M., Li, X., Zhang, G., Lo, P. G.-Q., and Kwong, D.-L., "Design guidelines of periodic Si nanowire arrays for solar cell application," *Appl. Phys. Lett.* 95(24), 243113 (2009).
- [23] Garnett, E., and Yang, P., "Light Trapping in Silicon Nanowire Solar Cells," *Nano Lett.* 10(3), 1082-1087 (2010).
- [24] Gunawan, O., Wang, K., Fallahzad, B., Zhang, Y., Tutuc, E., and Guha, S., "High performance wire-array silicon solar cells," *Prog. Photovoltaics* 19(3), 307-312 (2010).
- [25] Kelzenberg, M. D., Turner-Evans, D. B., Putnam, M. C., Boettcher, S. W., Briggs, R. M., Baek, J. Y., Lewis, N. S., and Atwater, H. A., "High-performance Si microwire photovoltaics," *Energ. Environ. Sci.* 4(3), 866-871 (2011).
- [26] Peng, K.-Q., Wang, X., Li, L., Wu, X.-L., and Lee, S.-T., "High-Performance Silicon Nanohole Solar Cells," *J. Am. Chem. Soc.* 132(20), 6872-6873 (2010).
- [27] Han, S. E., and Chen, G., "Optical Absorption Enhancement in Silicon Nanohole Arrays for Solar Photovoltaics," *Nano Lett.* 10(3), 1012-1015 (2010).
- [28] Lin, C., and Povinelli, M. L., "Optical absorption enhancement in silicon nanowire and nanohole arrays for photovoltaic applications," *Proc. of SPIE* 7772, 77721G (2010).
- [29] Wang, F., Yu, H., Li, J., Wong, S., Sun, X. W., Wang, X., and Zheng, H., "Design guideline of high efficiency crystalline Si thin film solar cell with nanohole array textured surface," *J. Appl. Phys.* 109(8), 084306 (2011).
- [30] Fan, S. H., and Joannopoulos, J. D., "Analysis of guided resonances in photonic crystal slabs," *Phys. Rev. B* 65(23), 235112 (2002).
- [31] Tikhodeev, S. G., Yablonskii, A. L., Muljarov, E. A., Gippius, N. A., and Ishihara, T., "Quasiguidded modes and optical properties of photonic crystal slabs," *Phys. Rev. B* 66(4), 045102 (2002).
- [32] Shockley, W., and Queisser, H. J., "Detailed balance limit of efficiency of p-n junction solar cells," *J. Appl. Phys.* 32(3), 510-519 (1961).
- [33] Kupec, J., Stoop, R. L., and Witzigmann, B., "Light absorption and emission in nanowire array solar cells," *Opt. Express* 18(26), 27589-27605 (2011).
- [34] Yamamoto, K., "Thin-film poly-Si solar cells on glass substrate fabricated at low temperature," *Appl. Phys. A: Mater.* 69, 179-185 (1999).
- [35] ASTM, <http://rredc.nrel.gov/solar/spectra/am1.5>
- [36] Li, M., "High-efficiency calculations for three-dimensional photonic crystal cavities," *Opt. Lett.* 31(2), 262-264 (2006).
- [37] Whittaker, D. M., and Culshaw, I. S., "Scattering-matrix treatment of patterned multilayer photonic structures," *Phys. Rev. B* 60(4), 2610-2618 (1999).
- [38] Edwards, D. F., "Silicon (Si)", *Handbook of optical constants of solids*, Academic, Orlando, Fla.(1985).
- [39] Kayes, B. M., Atwater, H. A., and Lewis, N. S., "Comparison of the device physics principles of planar and radial p-n junction nanorod solar cells," *J. Appl. Phys.* 97(11), 114302 (2005).
- [40] Kelzenberg, M., Putnam, M., Turner-Evans, D., Lewis, N., and Atwater, H., "Predicted efficiency of Si wire array solar cells," *Proc. of the 34th IEEE PVSC*, (2009).